THE EFFECT OF MOTION BLUR ON PHOTOGRAMMETRIC MEASUREMENTS OF A ROBOTIC MOVING TARGET

Mohammed A. Isa[1], Richard Leach[1,2], David Branson[1], and Samanta Piano[1]
[1]Manufacturing Metrology Team
Faculty of Engineering, University of Nottingham, Nottingham, UK
[2]Taraz Metrology, Nottingham, UK

MOTION BLUR

Photogrammetric measurement of a moving optical target can be prone to image distortion and blurring during acquisition. In high-precision optical tracking, where there is a relative motion between camera and target, image blur presents challenges to measurement accuracy because it can influence feature detection algorithms [1], which in turn, can alter three-dimensional (3D) coordinate measurements. In conventional photogrammetric systems, stable and sharp images are ensured by fixing the relative position between the camera and the measured target [2]. However, maintaining a static camera-target position during image acquisition is not possible in some applications, such as robotic tracking and unmanned air vehicle surveillance. In these situations, images should ideally be captured instantaneously. However, current technologies require the sensors to be exposed to light for some time to accumulate sufficient charge to build a high-intensity signal [3]. Furthermore, non-static photogrammetry applications require high-resolution, compact hardware and potentially multiple sensors, making the use of costly high-speed imaging disadvantageous and impractical. Motion blur effects occur when the shutter mechanism of a camera exposes its sensor to a moving scene, where the projected scene alters by more than the size of the sensor pixel during the exposure time. When the scene projection changes by tens of pixels, the blur effect is aggravated and localisation of features can become problematic. Consequently, blurred images can lead to erroneous photogrammetry results and the level of confidence in the measurement results is difficult to ascertain.

Most previous research on motion blur focuses on image restoration and camera stabilisation, where qualitative image improvement is emphasised, with less regard to how the 3D coordinate measurements obtained from the images are influenced [4]. Commonly, research on motion blur aims at improving image quality by estimating the image motion parameters and restoring the image quality using estimated point spread functions (PSFs) simplified as convolution kernels [5,6]. Imaging systems are fitted with motion sensors to better estimate movements, such as human hand jitters [7]. Even for a non-blind system, where the motion blur kernel is known, image deblurring can be complex and computationally expensive [5]. For metrological purposes, measurement precision and accuracy are fundamental and factors that influence blurring, such as the relative camera-target trajectory, need to be accurately measured.

By accurately measuring the displacement of a target with a laser interferometer, we investigate the effect of motion blur in a photogrammetry system. The idea is to use the controlled experimental environment to identify and characterise the image blurring phenomenon on a moving target before mounting the target on a robot. From the experiment, the performances of generated blur kernels are evaluated by comparing the acquired blurred images to their artificial counterparts derived from the static images of the targets. The measurement accuracy of the target is also evaluated for various camera-target displacements to obtain a basis for both a blur correction scheme and camera parameter selection. A significant reduction in measurement precision can be expected when motion blur increases in the images of measured targets [4]. Sieberth et al. [8] showed that an observed feature size increases exponentially as the scene-camera relative displacement increases during exposure. For photogrammetric systems that depend on the dimensions of features on an artefact, such as the robotic target in this paper, high displacements during exposure can easily render images unusable.

It is important for robotic target artefacts to allow six-dimensional (6D) pose tracking, which can be achieved by using target that has features with premeditated dimensions. [9]. As a result, when the target artefact is calibrated, it can serve as a

reliable reference for photogrammetric measurements. Successful tracking of these 6D targets depends on the ability to distinguish the dimensions of its features. Since blurring can distort sizes and dimensions of target features, it becomes necessary to investigate how 3D coordinate measurements of the target features are affected by motion blur.

EXPERIMENT

Displacements of a 6D robotic target were measured using both laser interferometry and photogrammetry. As an accurate and traceable benchmark for measuring displacements [10], the interferometry readings were used as reference for evaluating the performance of the photogrammetric measurements. Images of the target in motion were used to investigate motion blur and its effects on photogrammetric measurement.

Setup specifications

Three 20 mega-pixel Basler machine vision cameras were used to take images of the target. The parameters of the cameras were pre-calibrated using Zhang's method [11] and images were captured at 90 ms exposure time through 16 mm focal length lenses. In addition to individual cameras, multi-camera parameters defining image-based correspondences within the camera pairs were obtained. These parameters were used for the match selection and triangulation of identified features in obtained images.

The robotic target consists of eleven Polyoxymethylene spherical balls attached to dark contrasting plates (FIGURE 1). The size and spacing of the spheres were designed to reinforce identification at all possible poses. Dimensions of the target, such as sphere diameters and spacings, have been traceably measured using a mechanical coordinate measuring machine. For this study, the target was fixed to a linear actuator stage that moves in a single direction as shown in FIGURE 1. Kinematic errors in the two linear and three angular constrained degrees of freedoms were neglected. As justification for the simplification, the magnitude of the corresponding errors from the constrained motion have been shown to be less 10 μm for a linear actuator of similar build [12].

A Renishaw XL-80 laser interferometer was used to determine the displacements of the linear actuator. As illustrated in FIGURE 1, a retroreflector was placed on the moving actuator stage while the interferometer optical components were rigidly fixed to the optical table. Displacement measurement accuracy of 0.2 μm is given by the manufacturer for the measurement range of 300 mm. The linear actuator is open-loop controlled and its movement is synchronised with data collection from both the laser interferometer and the photogrammetric system.

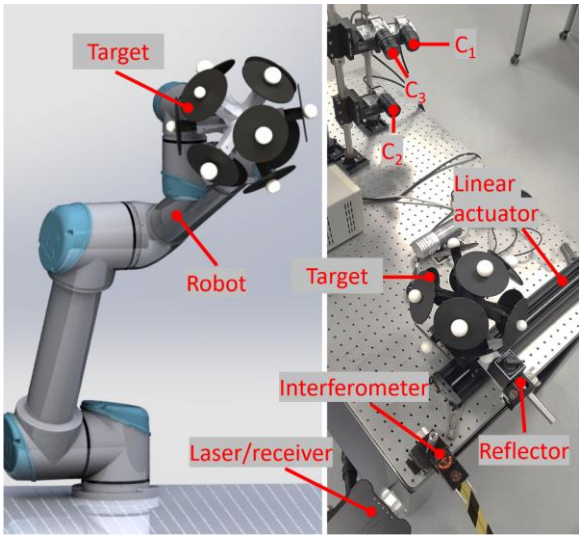

FIGURE 1. A photogrammetric target designed for use on a collaborative robot is placed on a linear actuator where displacement is measured with a linear interferometer. Three cameras C_1, C_2 and C_3 are used to capture images of the target.

Motion speed test

It is important to ensure that the motion of the target artefact is well characterised when the cameras are triggered to acquire images. To ensure that a desired speed is attained, the maximum speed setting of the actuator was varied from 500 mm min^{-1} to 6000 mm min^{-1} and displacements were recorded at 0.1 s time intervals. FIGURE 2 shows that the desired speed settings were attained in each case at around 0.2 s. The maximum speed of 6000 mm min^{-1} was reached when the total displacement was around 30 mm. Based on this finding, the cameras were set to be triggered at 0.25 s after the linear actuator starts moving and a displacement interval of 30 mm or more was used for the speed settings above. Images acquired in the motion blur experiments given in this paper were taken in the exposure time window shown in FIGURE 2.

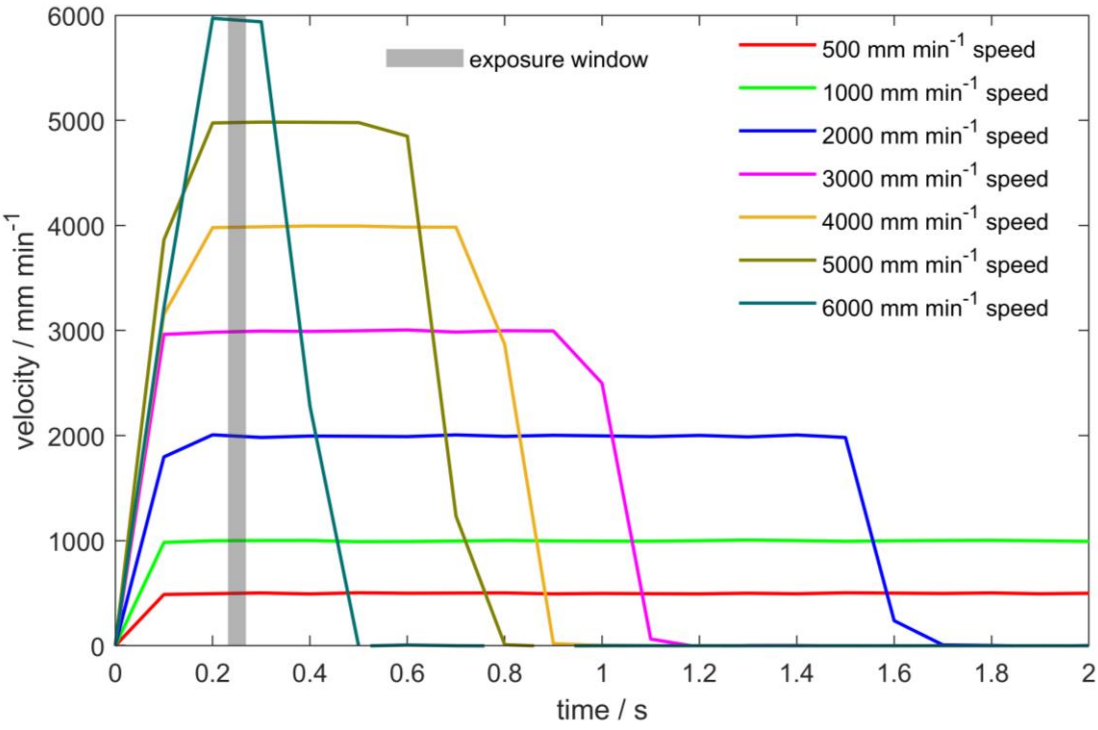

FIGURE 2. Measured velocity profiles at various maximum speed settings. The velocities are derived from measured displacements at 0.1 s intervals from the laser interferometer.

Motion blur experiment

Two sets of images were obtained for the motion blur experiment at camera measurement depths of around 600 mm to 800 mm. The first set contains images of the moving target captured at 500 mm min^{-1} to the maximum speed of 6000 mm min^{-1}. Immediately after the three cameras were triggered, before the image frames were fully formed, displacement readings from the laser interferometer were taken. The target was then brought to rest after a 30 mm displacement and the process was repeated, until the total travel distance of 300 mm was reached. For the second set of images, another run was initiated, but this time, the linear actuator was displaced to the exact locations recorded during the first run. The target was allowed to rest at this location before the images were taken. Hence, the second set of images represent the static counterparts of the first set of images. The average time it took to trigger the three cameras was 8.4 ms and the time elapsed to request a reading from the laser interferometer was 3.5 ms.

PHOTOGRAMMETRY

Photogrammetric measurement provides the overall configuration and 3D location of the experimental setup. Knowing the speed of the moving target is not sufficient to determine the form of image blur. Objects moving at different orientations or positions will be blurred differently. It is, therefore, necessary to determine the 3D location and motion direction of the desired features relative to the cameras.

Multi-view stereo correspondence

The network of three stereo-camera pairs (C_{12}, C_{13}, C_{23}) is formed and the correspondence between the image points from each stereo pair is determined by a fundamental matrix. For a camera pair where the first camera C_i and second camera C_j are characterised by the fundamental matrix $\boldsymbol{F}_{ij}$, two matching image points $\boldsymbol{x}_i$ and $\boldsymbol{x}_j$ from the first and the second camera respectively should reduce the epipolar relationship $\epsilon_{ij} = \boldsymbol{x}_j^T \cdot \boldsymbol{F}_{ij} \cdot \boldsymbol{x}_i$ to zero. Here, the two image points are expressed in homogenous coordinates [13]. Due to digital noise and other sources of error, it is normally difficult to obtain $\epsilon_{ij} = 0$ exactly from a set of candidate image points [14]. A practical approach is to choose a threshold ϵ_m such that matches are accepted only if $\epsilon_{ij} < \epsilon_m$. In this paper, ϵ_m is determined from a maximum allowable image pixel deviation. The pixel

deviations can be obtained by normalising ϵ_{ij} based on each epipolar line in $\boldsymbol{F}_{ij} \cdot \boldsymbol{x}_i$.

Once the image points are matched, triangulation of the matches reconstructs the 3D points. The measured 3D points correspond to the centres of the target spheres. Beside the centre points, diameters of the spheres are estimated from the stereo images. The collection of distances and diameters reconstructed from each frame of the three cameras are cross-referenced with the CMM-measured dimensions of the target.

Evaluation of image blur length and orientation

3D locations of identified target artefact spheres are used to determine the motion direction of the stage. The motion direction $\boldsymbol{v}_m$ expressed as a unit vector, can be used to determine the change in the image centre points of the target spheres. For a measured 3D centre of a sphere $\boldsymbol{p}$ moving with speed s, the image projection of its centre after the exposure time t_e is given by

$$\boldsymbol{x_b} = \boldsymbol{K} \cdot [\boldsymbol{R}|\boldsymbol{t}] \cdot (\boldsymbol{p} + st_e\boldsymbol{v}_m), \quad (1)$$

where $\boldsymbol{K}$ is camera intrinsic matrix, and $\boldsymbol{R}$ and $\boldsymbol{t}$ are the respective rotation and translation of the origin of $\boldsymbol{p}$ with respect to the camera origin. The change in image projection of a point moving in a straight line can be obtained from Equation (1) as $\Delta\boldsymbol{x_b} = \boldsymbol{K} \cdot [\boldsymbol{R}|\boldsymbol{t}] \cdot st_e\boldsymbol{v}_m$. The magnitude and direction of $\Delta\boldsymbol{x_b}$ determines the motion blur kernel used in this study. The motion blur kernel, generated using the MATLAB image processing toolbox, serves as the shift-invariant PSF of the motion blur.

RESULTS

Reconstructed points are used to determine the displacement error of the photogrammetry system. Generated blurred images of the target spheres are also analysed.

Displacement error

Step displacements at the image acquisition intervals of the motion blur experiment were evaluated from the 3D reconstructed points of matched sphere centres. Displacement errors were obtained by subtracting the reference laser interferometer displacement from the photogrammetric displacement in each step. The displacements of spheres that match both the multi-view stereo criteria and the internal spatial conditions of the target are computed. Ensuring both matches are satisfied reduces the likelihood of error in matching.

FIGURE 3 gives the mean displacement error for the three camera pairs with error bars indicating the maximum and minimum error at the linear actuator positions given as the abscissa of the graphs. Due to reliance of the identification algorithm on the internal spatial matching of the target spheres, the number of successful sphere centre reconstructions began to drop below three at the speed of 1000 mm min^{-1}. In FIGURE 3a), for the speed of 1000 mm min^{-1}, there were no 3D points reconstructed at the linear actuator position of 240 mm and above. A similar case was observed for speeds of 2000 mm min^{-1} to 6000 mm min^{-1}. At these high speeds, the image acquired was too degraded for the detection and identification algorithm using similar thresholding parameters with the static images. Future work will investigate integrating colour invariants and background modelling [15] to isolate a target so that some of the detection parameters can be relaxed.

The mean error from the static images shown in FIGURE 3 are less than 80 µm throughout the experiment. The maximum mean error increases to around 100 µm for images captured at 500 mm min^{-1} with the error range observed to increase significantly too. At the speed of 1000 mm min^{-1}, some mean errors approach 600 µm, and in some cases, the measured displacement error exceeds 1 mm.

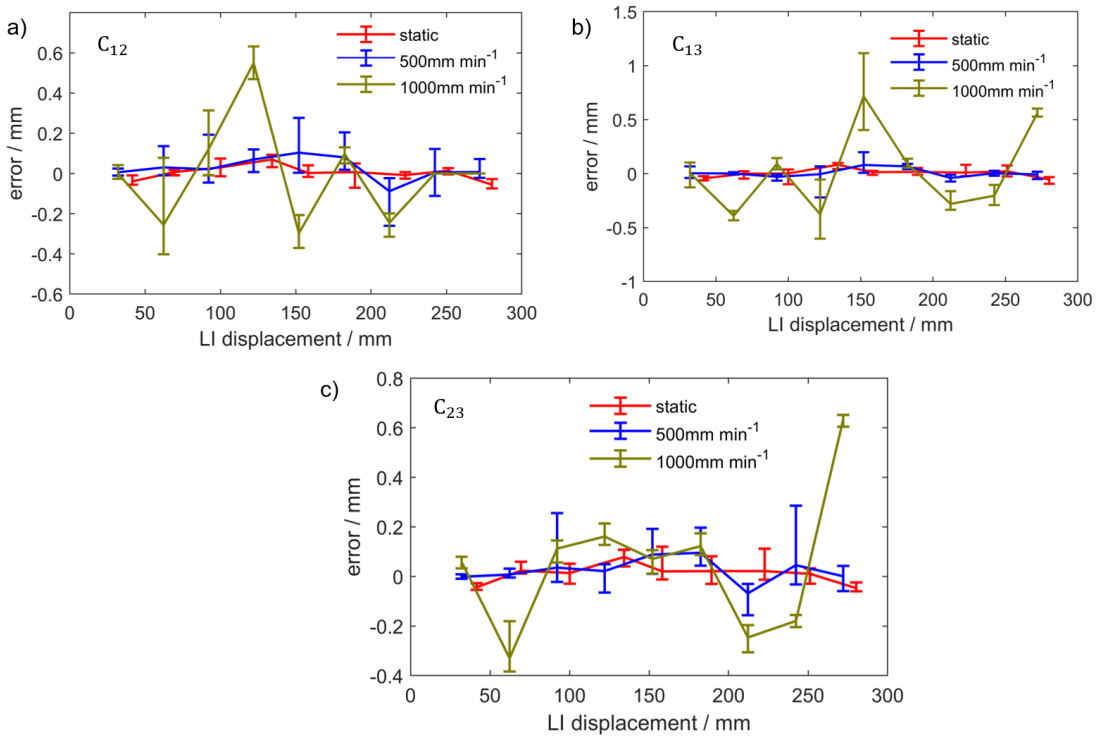

FIGURE 3. Displacement errors for subsequent image acquisition intervals of the photogrammetry system are given. Errors from stereo-camera pairs C_{12}, C_{13} and C_{23} are given in 3(a), 3(b) and 3(c) respectively. Reference displacements are obtained from the laser interferometer (LI).

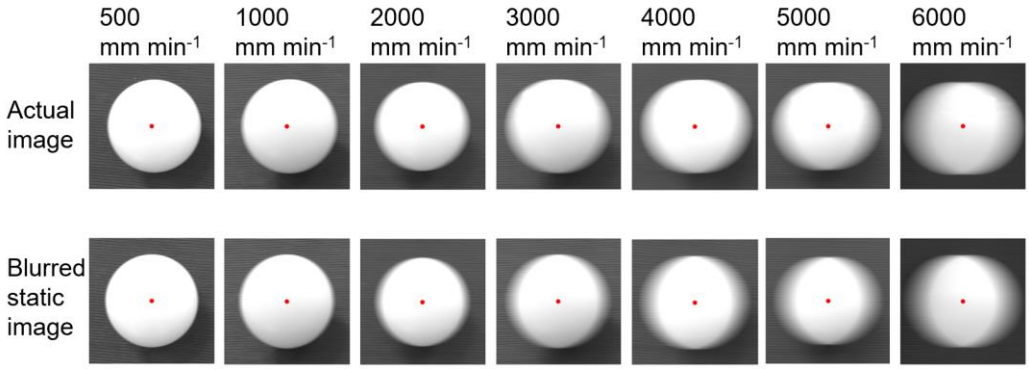

FIGURE 4. Generated blurred images at detected target spheres are compared with the actual images captured from the camera at different speed settings.

Generation of motion blur

Blurring reduces the sharpness of images, therefore, reducing high gradient and frequency features in the spatial and frequency domains of images respectively. Most detection algorithms, such as edge detection-based methods, rely on these high gradient (and high spatial frequency) features and are, therefore, affected when an image is blurred. Specific to this study, sphere edges in severely blurred images do not meet some criteria, such as, having a minimum radial gradient value and are, therefore, undetected. FIGURE 4 compares the blurring effect on the actual images captured in motion with the generated blur on static images.

A quantitative analysis of the image regions of the matched spheres is given in FIGURE 5 as mean-squared errors (MSEs) of the blurred static images. The MSE is the measure of the difference between the pixel intensities of the generated blurred images and the actual moving

images captured. Both images are 8-bit quantised and padded on each side of the detected sphere by 60 pixels. The MSE is mostly below 1000, except for images obtained at 6000 mm min^{-1}. At the maximum speed, sphere centre positions in the two images compared vary significantly.

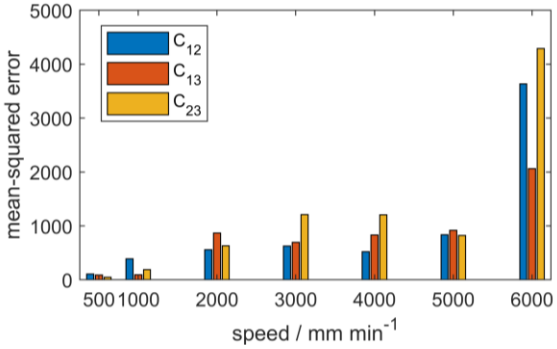

FIGURE 5. Mean-squared error of generated blurred spheres evaluated from the actual images captured in motion.

CONCLUSION

This paper investigates the effect of motion blur on the photogrammetric measurement of a 6D robotic target. 3D coordinate measurement of the moving target is investigated using reference laser interferometer measurements. It is observed that photogrammetric 3D measurement is possible when the target moves at speeds below 1000 mm min^{-1}. In addition, accurately measured displacements of the target are used to simulate blurred images that are comparable with the actual moving images. Further research will investigate more complex motion and devise computationally efficient strategies that can reduce the error caused by image blurring.

Acknowledgments: This work is funded by the Engineering and Physical Sciences Research Council (EPSRC) under grant number: EP/T023805/1—High-accuracy robotic system for precise object manipulation (HARISOM).

REFERENCES

[1] Mei C, Reid I. Modeling and generating complex motion blur for real-time tracking. 2008 IEEE Conf. Comput. Vis. Pattern Recognit., IEEE; 2008.

[2] Sims-Waterhouse D, Leach R K, Piano S. Close-range photogrammetry. Advanced Optical Form and Coordinate Metrology, IOP Publishing; 2020, p. 4–18.

[3] Luo Y, Ho D, Mirabbasi S. Exposure-programmable CMOS pixel with selective charge storage and code memory for computational imaging. IEEE Trans. Circuits Syst. I Regul. Pap. 2018;65:1555–66.

[4] Yang H, Yi Y, Liu G, Shi X. CS-BS-EF: An integrated method for tracking flying ping-pong with motion blur. Proc. 2013 Int. Conf. Mechatron. Sci. Electr. Eng. Comput., 2013, p. 1220–3.

[5] Rajagopalan A N, Chellappa R, editors. Motion Deblurring: Algorithms and Systems. Cambridge University Press; 2014.

[6] Zhao H, Shang H, Jia G. Simulation of remote sensing imaging motion blur based on image motion vector field. J. Appl. Remote Sens. 2014;8:083539.

[7] Yang C, Feng H, Xu Z, Chen Y, Li Q. Image deblurring utilizing inertial sensors and a short-long-short exposure strategy. IEEE Trans. Image Process. 2020;29:4614–26.

[8] Sieberth T, Wackrow R, Chandler J. Influence of blur on feature matching and a geometric approach for photogrammetric deblurring. Int. Arch. Photogramm. Remote Sens. Spat. Inf. Sci. 2014;XL–3:321–6.

[9] Pintaric T, Kaufmann H. A rigid-body target design methodology for optical pose-tracking systems. Proc. 2008 ACM Symp. Virtual Real. Softw. Technol.; 2008.

[10] Isa M A, Sims-Waterhouse D, Piano S, Leach R K. Volumetric error modelling of a stereo vision system for error correction in photogrammetric three-dimensional coordinate metrology. Precis. Eng. 2020;64:188–99.

[11] Zhang Z. A Flexible New Technique for Camera Calibration. IEEE Trans. Pattern Anal. Mach. Intell. 2000;22:1330–4.

[12] Isa M A, Sims-waterhouse D, Piano S, Leach R K. Kinematic error analysis of stage tracking using stereo vision. Proc. ASPE, 2019.

[13] Guan B, Yu Y, Su A, Shang Y, Yu Q. Self-calibration approach to stereo cameras with radial distortion based on epipolar constraint. Appl. Opt. 2019;58:8511–21.

[14] Zhou H, Chen Y, Feng R. A novel background subtraction method based on color invariants. Comput. Vis. Image Underst. 2013;117:1589–97.